





Article

Technical and Economic Evaluation for Off-Grid Hybrid Renewable Energy System Using Novel Bonobo Optimizer

Hassan M. H. Farh ^{1,*} , Abdullrahman A. Al-Shamma'a ^{2,*} , Abdullah M. Al-Shaalan ², Abdulaziz Alkuhayli ² ,
Abdullah M. Noman ²  and Tarek Kandil ³

- ¹ Faculty of Construction and Environment, Department of Building and Real Estate, Hong Kong Polytechnic University, Hung Hom, Kowloon, Hong Kong
- ² Department of Electrical Engineering, College of Engineering, King Saud University, Riyadh 11421, Saudi Arabia; shaalan@ksu.edu.sa (A.M.A.-S.); aalkuhayli@ksu.edu.sa (A.A.); anoman@ksu.edu.sa (A.M.N.)
- ³ Department of Electrical and Computer Engineering, College of Engineering and Computing, Georgia Southern University, Statesboro, GA 30460, USA; thassankandil@georgiasouthern.edu
- * Correspondence: hfarh.hussein@polyu.edu.hk (H.M.H.F.); ashammaa@ksu.edu.sa (A.A.A.-S.)

Abstract: In this study, a novel bonobo optimizer (BO) technique is applied to find the optimal design for an off-grid hybrid renewable energy system (HRES) that contains a diesel generator, photovoltaics (PV), a wind turbine (WT), and batteries as a storage system. The proposed HRES aims to electrify a remote region in northern Saudi Arabia based on annualized system cost (ASC) minimization and power system reliability enhancement. To differentiate and evaluate the performance, the BO was compared to four recent metaheuristic algorithms, called big-bang–big-crunch (BBBC), crow search (CS), the genetic algorithm (GA), and the butterfly optimization algorithm (BOA), to find the optimal design for the proposed off-grid HRES in terms of optimal and worst solutions captured, mean, convergence rate, and standard deviation. The obtained results reveal the efficacy of BO compared to the other four metaheuristic algorithms where it achieved the optimal solution of the proposed off-grid HRES with the lowest ASC (USD 149,977.2), quick convergence time, and fewer oscillations, followed by BOA (USD 150,236.4). Both the BBBC and GA algorithms failed to capture the global solution and had high convergence time. In addition, they had high standard deviation, which revealed that their solutions were more dispersed with obvious oscillations. These simulation results proved the supremacy of BO in comparison to the other four metaheuristic algorithms.

Keywords: hybrid renewable energy system; bonobo optimizer; annualized system cost; optimal solution; convergence rate; renewable energy fraction; artificial intelligent algorithms



Citation: Farh, H.M.H.; Al-Shamma'a, A.A.; Al-Shaalan, A.M.; Alkuhayli, A.; Noman, A.M.; Kandil, T. Technical and Economic Evaluation for Off-Grid Hybrid Renewable Energy System Using Novel Bonobo Optimizer. *Sustainability* **2022**, *14*, 1533. <https://doi.org/10.3390/su14031533>

Academic Editor: Mohamed A. Mohamed

Received: 28 December 2021

Accepted: 20 January 2022

Published: 28 January 2022

Publisher's Note: MDPI stays neutral with regard to jurisdictional claims in published maps and institutional affiliations.



Copyright: © 2022 by the authors. Licensee MDPI, Basel, Switzerland. This article is an open access article distributed under the terms and conditions of the Creative Commons Attribution (CC BY) license (<https://creativecommons.org/licenses/by/4.0/>).

1. Introduction

Renewable energy resources, unlike conventional generation resources, are inexhaustible and lasting sources of energy. The world requires renewable and reliable energy resources since they are much cleaner and produce energy without the harmful effects of pollution [1,2]. There are different renewable energy generation sources, like wind turbines (WT), solar photovoltaics (PV), biomass energy, geothermal energy, etc. Besides their advantages, such as being environmental friendly, sustainability, etc., wind energy and solar PV energy have been used frequently due to the reduction in their manufacturing cost and growing industrial and residential applications [3]. These sources can be used individually or connected as a hybrid to feed power to the grid. In addition, renewable energy sources can be used to electrify remote areas, which considered off-grid loads and are unable to be supplied from an attainable grid. Due to the non-reliability and excessive sizing of using a single source (e.g., PV) to feed power to off-grid areas, hybrid renewable energy resources are proposed to meet these challenges [4]. Hybrid renewable energy systems (HRES) can comprise PVs, WT, diesel generators, batteries, fuel cells (FCs), etc. However, due to the

nonlinear and random operation of renewable energy resources, challenges arise when they are used to electrify off-grid loads [5,6]. The challenges include reduced reliability, more control complexity, design and sizing considerations, unstable and less energy, etc. These challenges represent complex and nonlinear optimization problems. Optimization means reaching the optimal solution and the best design of the HRES with minimum cost [7,8].

There are numerous optimization algorithms that have been used to search for the optimal sizing of hybrid renewable energy systems, including traditional algorithms, artificial intelligence (soft computing) algorithms [9–17], hybrid algorithms [4,6,18], and software tools [19–23]. Traditional algorithms can be classified as analytical algorithms [24–27], graphical algorithms [28,29], probabilistic algorithms [24,30,31], and numerical techniques [32]. Traditional techniques are simple. However, they have certain requirements to define the optimization problem. For example, graphical techniques depend on the solar irradiance and wind speed to determine the sizing of the HRES, which causes over sizing or under sizing [33]. Analytical algorithms cannot deal with many resources and may consume more computational time compared to AI algorithms. On the other hand, other techniques such as soft computing techniques, hybrid, and software tools have no specific requirements like traditional techniques, which leads to solving the optimization problems effectively. Consequently, this literature focuses on software tools, hybrid, and soft-computing techniques.

Spreading the use of HRES to electrify rural on-grid/off-grid areas motivated researchers to explore more technical and economic feasibility issues. A techno-economic analysis was implemented using the HOMER PRO software tool in [20–23]. The authors in [20] studied, analyzed, and designed the techno-economic feasibility of a solar PV–diesel–battery energy system to electrify a village in Pakistan, taking the availability time of the grid as a constraint. The optimal sizing and the techno-economic feasibility were carried out using HOMER PRO software. The findings of this study revealed that the levelized cost of electricity (LCOE) in on-grid HRES is more economical than off-grid HRES. In [21], a study was developed using the HOMER PRO software tool to redesign and refinance a remote HRES (solar PV, diesel, and battery) on a small island in Thailand. The HRES was optimized to attain the lowest cost of electricity. In [22], a study was carried out to study the electrification of a rural community in Benin. The study found that the hybrid solar PV–diesel–battery system attained the lowest cost optimal system.

As mentioned above, optimal sizing of an HRES is unavoidable since over-sizing results in increasing the initial cost and under sizing may result in reducing the shared power from the HRES and consequently reducing system reliability. Recently, great attention has been centered on studying the optimal sizing of an HRES. Some of the published studies focused on a single objective mathematical model and others focused on multi-objective models [13,34–36]. The authors in [34] developed a model based on fuzzy logic to minimize the annualized cost of the HRES that encompasses solar PV–WT–battery. The authors in [13] utilized a genetic algorithm (GA) to find the optimal sizing of an HRES in power distribution networks based on minimizing the power losses and the expected energy not supplied. The authors in [35] used GA for optimal sizing for a hybrid PV–WT–battery system integrated into the energy management strategy. The energy management was attained based on a proposed economic model predictive control approach [12]. The authors in [36] combined a quasi-steady operational method and GA for optimal sizing of a solar PV–pump storage hydroelectric energy system based on investment cost and loss of power supply probability (LPSP) as an objective function. In [37], a MATLAB model was developed for the optimal design of a wind–hydro system based on reduction the cost of energy (COE) and CO₂ emissions. The authors in [38] applied a crow search algorithm for the optimal sizing of an autonomous microgrid including PV–WT to supply a research center based on the annual system cost. In [39], particle swarm optimization (PSO) technique-based Monte Carlo simulation was employed to reach the optimal size of a solar PV–WT–battery based on minimizing the total annual cost (TAC). In [40], GA was used to find a multi-objectives sizing solution for a solar PV–WT–solar collector–battery system based on minimizing the net present cost (NPC). The authors in [41] utilized the Pareto evolutionary algorithm to

minimize the LCOE and the CO₂ life cycle emissions (LCE) for a solar PV–WT–DG–battery standalone system. In [42], a water cycle algorithm in addition to moth-flame optimization were used for the techno-economic optimal design of a solar PV–biogas generator–pumped hydro energy storage–battery energy system. The objective function was a minimization of TNPV. The water cycle and moth-flame optimizer techniques were compared and assessed with the GA. The authors in [43] introduced the differential evolution algorithm (DEA) incorporated with the fuzzy technique to optimally design a solar PV–WT–DG–hydrogen–battery energy system based on minimum cost, emissions, and unmet load. An improved fruit fly optimizer technique was proposed by [44] to optimally design a hybrid solar PV–WT–diesel–battery system based on minimizing the TAC and the pollutant emission. The authors in [45] utilized a line-up competition algorithm (LUCA) to determine the optimal design of a solar PV–WT–DG–battery energy system based on minimizing the TAC and CO₂ emissions. The authors in [17] proposed a cuckoo search (CS) technique for the optimal design of three HRESs: solar PV–battery, WT–battery, and solar PV–WT–battery systems, minimizing total system cost. This algorithm was compared to the PSO and GA algorithms, and the results show that CS gave better solutions and faster convergence. The author in [46] utilized the grey wolf optimization algorithm for the optimal design of an HRES encompassing a PV–WT–biomass system based on minimizing the TNPC and LPSP. The findings obtained by GWO were compared to the findings obtained by GA and simulated annealing (SA) algorithms, and the superiority of the GWO was confirmed. The authors in [47] introduced a hybrid Big Bang–Big Crunch (BBBC) technique for the optimal sizing of a solar PV–WT–battery standalone HRES. In [48], the authors utilized the ant colony optimization (ACO) based integer continuous domain programming to optimally size a PV–WT system based on minimizing the TAC.

Based on the preceding literature review, metaheuristic algorithms proved their efficacy and robustness to deal with the optimal design optimization problem of an HRES in comparison to the analytical and graphical ones. Therefore, this study proposes a novel bonobo optimizer (BO) algorithm, which was applied to search for the optimal design of the proposed off-grid HRES to electrify an urban region located in northern Saudi Arabia. The main novelty and contributions of this study are manifested as shown below:

- A novel BO algorithm was applied for the first time in this research to find the optimal design of the proposed off-grid HRES based on minimizing the annualized system cost and enhancing the power system reliability level.
- Technical and economic evaluation were attained for the proposed off-grid HRES that includes PV, WT, diesel, and batteries to electrify an urban region in northern Saudi Arabia, namely, Al Sulaymaniyah.
- To validate the performance soundness and credibility, the BO algorithm was compared to other four metaheuristic algorithms, namely, BBBC [47], GA [35], crow search [38], and the butterfly optimization algorithm (BOA) [49] in terms of optimal and worst solutions captured, mean, standard deviation (STDEV), convergence rate, and oscillations around steady state.
- The simulation results revealed the supremacy performance of the BO algorithm compared to the other four metaheuristic algorithms. It attained the optimal design of the HRES with the minimum ASC (USD 149,977.2), quick convergence time, and fewer oscillations, followed by BOA (USD 150,236.4). The BBBC and GA algorithms failed to capture the global solution and had high STDEV, high oscillations, and high convergence time.

This research paper is organized as follows: Section 2 describes the proposed off-grid HRES components and their mathematical modeling. In Section 3, the problem formulation is covered, including the objectives, constraints, and the proposed BO algorithm for HRES optimal sizing. Section 4 covers the simulation results, analysis, and discussions. Finally, Section 5 epitomizes the conclusions.

2. Description of the Proposed Off-Grid Hybrid Renewable Energy System

The proposed HRES under study is shown in Figure 1. This HRES encompasses two renewable sources—solar PV and WT—in addition to the diesel generator and battery banks for energy storage. Both solar PV arrays and batteries are interconnected directly to the DC busbar, whereas the WT and the diesel are interconnected to the AC busbar, as demonstrated in Figure 1 below. The bidirectional DC/AC converter has two jobs. The first job is converting the AC to DC, where it works as a bridge rectifier in this process. The second job is converting the DC to AC, and it works as an inverter in this job. The batteries are used to cover and supply the load once the renewable resources are not capable of supplying the required load demand. The diesel generators are the second standby generation source, which are used in case the renewables are not available and the energy stored in the batteries is consumed. The mathematical modeling of the HRES components under study are demonstrated in the following sections.

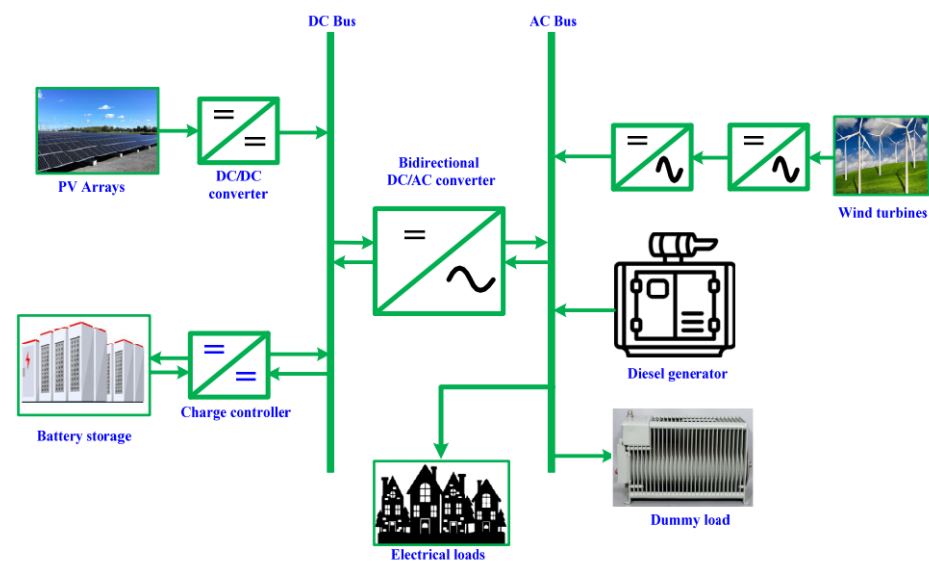


Figure 1. The hybrid renewable energy system (HRES) under study.

2.1. Modeling of PV Generation Source

The output power captured from the PV modules (P_{PV}) as a function of the PV rated power is [50]:

$$P_{PV} = P_r f_{PV} \left(\frac{\overline{G_T}}{\overline{G_{T,STC}}} \right) [1 + \alpha_P (T_c - T_{c,STC})] \quad (1)$$

where P_r is the PV rated power; $\overline{G_{T,STC}}$ and $\overline{G_T}$ are the solar PV radiation for standard test conditions (STCs) and normal conditions, respectively; $T_{c,STC}$ and T_c are the temperatures under STCs and normal conditions, respectively; and α_P and f_{PV} are the power temperature coefficient and derating coefficient, respectively. The PV steady-state temperature is formulated as shown below [50].

$$T_c = \frac{T_a + (NOCT - T_{a,NOCT})(1 - 1.11\eta_{MPP}(1 - \alpha_P T_{c,STC})) \left(\frac{\overline{G_T}}{\overline{G_{T,NOCT}}} \right)}{1 + 1.11(\alpha_P \eta_{MPP,STC})(NOCT - T_{a,NOCT}) \left(\frac{\overline{G_T}}{\overline{G_{T,NOCT}}} \right)} \quad (2)$$

where

T_a and $NOCT$ are the cell temperature at ambient and nominal operating, respectively.
 $T_{a,NOCT}$ and $G_{T,NOCT}$ are the ambient temperature and solar PV radiation under nominal operating, respectively;

$\eta_{MPP,STC}$ and η_{MPP} are the PV MPP efficiency under STCs and normal conditions, respectively.

Each PV energy system is equipped with a maximum power point tracker (MPPT) device, which is used to extract the maximum power captured from the PV system by controlling the duty cycle of the DC/DC converter. The metaheuristic MPPT techniques proved their efficacy and accuracy in comparison to the conventional techniques to deal with both the normal and partial shading cases. The conventional techniques gave acceptable performance under uniform conditions but may have trapped to the local peak under partial shading.

2.2. Modeling of the WT Generation System

As demonstrated in Figure 2, the wind turbine starts to generate the output power once the wind speed exceeds the cut-in speed (u_c). At the rated speed (u_r), the wind power reaches its rated value till the cut-off or furling speed (u_f), where the wind turbine stops running if the wind speed exceeds its cut-off speed value. The output power captured by the WT depends on P_r , u_c , u_r , and u_f , which can be formulated as shown below [51].

$$P_{WT}(u) = \begin{cases} 0 & u < u_c \text{ or } u > u_f \\ P_r \times \frac{u^2 - u_c^2}{u_r^2 - u_c^2} & u_c \leq u \leq u_f \\ P_r & u_r \leq u \leq u_f \end{cases} \quad (3)$$

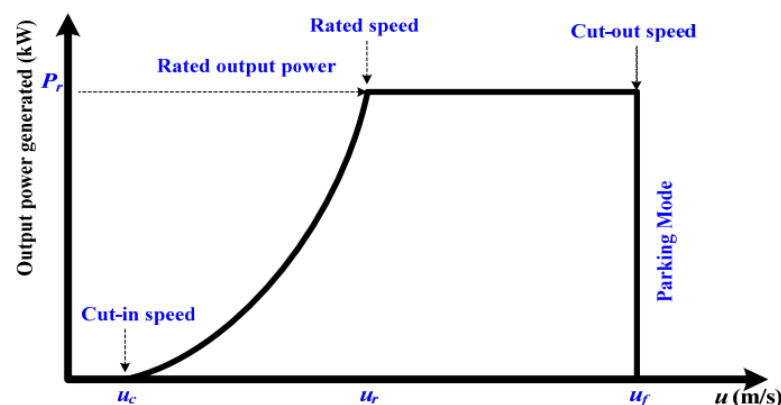


Figure 2. The WT power generated versus the wind speed characteristics.

2.3. Modeling of the Battery Bank as a Storage System

As a result of the intermittent nature of the renewable generation sources, whether WT or PV, the battery bank is considered a compulsory component in the HRES. They act as a storage element for the extra energy and supply it in case of deficiency by the WT and PV. The batteries will be in charging mode if the generated output power from the renewables (WT and PV) is higher than the demand, whereas they will be in discharging mode if the generated output power from the renewable sources is lower than the demand. The state of charge (SOC) or the charging power of the batteries at time t can be calculated with the following formula [52].

$$SOC(t) = SOC(t-1)(1 - \sigma) + \left(E_{GA}(t) - \frac{E_L(t)}{\eta_{inv}} \right) \eta_{Bat}. \quad (4)$$

where

σ is the hourly self-discharging rate;

$E_L(t)$ is the total demand;

$E_{GA}(t)$ is the total output power;

η_{inv} is the inverter efficiency;

η_{Bat} is the battery bank efficiency.

During the discharging mode, the SOC must be more than or equal to the minimum allowable limit (SOC_{min}), whereas it must not exceed the maximum allowable limit (SOC_{max}) during the charging mode. These modes or cases are expressed as follows:

$$SOC(t) = \begin{cases} SOC_{min} & SOC(t) < SOC_{min} \\ SOC(t) & SOC_{min} < SOC(t) < SOC_{max} \\ SOC_{max} & SOC(t) > SOC_{max} \end{cases} \quad (5)$$

2.4. Modeling of the Diesel Generator

The diesel generator is considered the secondary standby generation source, which is utilized to cover the load if the renewables (WT and PV) and the batteries are not capable of covering the load demand. The annual fuel cost depends on the diesel rated power and output power generated, which can be formulated as follows [50]:

$$C_{Diesel} = C_F \sum_{t=1}^{8760} A \times P_{Diesel}(t) + B \times P_R \quad (6)$$

where

C_F is the fuel cost per liter;

A and B are the fuel constants;

P_R and $P_{Diesel}(t)$ are the diesel rated power and output power generated at time t , respectively.

3. Problem Formulation: Objectives and Constraints

The proposed BO technique is applied for the optimal design/sizing of the proposed HRES, including solar PV , WT , diesel, and batteries. The objective of the HRES sizing optimization problem is to minimize the total annualized system cost (ASC) at an acceptable limit of reliability, taken as loss of power supply probability ($LPSP$). The objective function, in addition to the constraints of this optimization problem, can be summarized as follows:

$$\text{subject to : } \begin{cases} \text{Min } ASC, \\ LPSP \leq LPSP_{desired} \\ REF \leq REF_{desired} \\ 0 \leq P_{PV} \leq P_{PV,max} \\ 0 \leq P_{WT} \leq P_{WT,max} \\ P_{Bat.,min} \leq P_{Bat.} \leq P_{Bat.,max} \\ P_{Diesel,min} \leq P_{Diesel} \leq P_{Diesel,max} \end{cases} \quad (7)$$

where $LPSP_{desired}$ is the predetermined limit of $LPSP$, which gives an indication about the reliability, and $REF_{desired}$ is the predetermined limit of the renewable energy fraction (REF).

Based on the minimum ASC , the proposed BO algorithm will determine the optimal sizing of the solar PV , WT , diesel, and battery bank as follows:

$$x = [P_{PV}, P_{WT}, P_{Diesel}, P_{Bat.}] \quad (8)$$

where

P_{PV} , and P_{WT} are the optimal sizing in kW of PV and WT , respectively;

P_{Diesel} and $P_{Bat.}$ are the diesel rated power in kW and the capacity of battery in kWh, respectively;

$P_{PV,max}$, $P_{WT,max}$, $P_{Bat.,max}$, and $P_{Diesel,max}$ are the maximum power limit of the PV , WT , batteries, and diesel, respectively.

The ASC equals the annualized capital costs ($C_{Cap.}$), plus the O&M cost ($C_{O\&M}$) and annualized replacement costs ($C_{Rep.}$), as follows [50]:

$$ASC = C_{Cap.} + C_{O\&M} + C_{Rep.} \quad (9)$$

The total capital cost is expressed as follows [50]:

$$C_{Cap.} = (C_{Ren.} + C_{Bat.} + C_{Diesel}) \frac{i(1+i)^{Y_{proj}}}{(1+i)^{Y_{proj}} - 1} \quad (10)$$

where $C_{Ren.}$, $C_{Bat.}$, and C_{Diesel} are the capital costs of the renewable resources, battery bank, and diesel, respectively.

The annualized replacement cost can be formulated as shown below [50].

$$C_{Rep.} = C_{Rep.} \frac{i}{(1+i)^{Y_{rep}} - 1} \quad (11)$$

where $C_{Rep.}$ is the capital replacement cost and Y_{rep} is the lifetime of each component.

The LPSP can be defined as the power supply loss potential, which means that the HRES is not capable of supplying the load demand. On the other hand, it can be estimated by the percentage of the energy deficit of the total energy production of the HRES. Therefore, the LPSP gives us indication about the performance of the proposed HRES in terms of reliability and can be formulated as follows [50]:

$$LPSP = \frac{\sum_{t=0}^T \text{Power Failure Time (PFT)}}{T} \quad (12)$$

The *PFT* is the time interval during which the load cannot be supplied. An LPSP that equals 0% means that the load will be supplied all the time (T) and 100% LPSP means that the load cannot be supplied all the time (T).

The *REF* represents the energy portion submitted to the load demand that was generated by renewable generation sources and can be expressed as follows:

$$REF = \left(1 - \frac{E_{L,Diesel}}{E_{L,served}}\right) \times 100 \quad (13)$$

where $E_{L,Diesel}$ represents the total load supplied by diesel. The REF changes from 0% to 100%. A REF of 0% means that the diesel generator only supplies the load and no renewables, and 100% means that the load is supplied only by renewables. Therefore, the REF changes between 0% and 100%, which means that the power supplied is the result of sharing all renewable and non-renewable generation sources.

4. Application of Bonobo Optimizer Technique for HRES Optimal Sizing

The bonobo optimizer (BO) is a new meta-heuristic technique that is influenced by bonobos' reproductive strategy and social behavior. Das et al. developed a population-based method [53]. For efficient optimization, the algorithm uses bonobos' fission–fusion search approach. Bonobos divide into smaller groups known as fissions for the purpose of locating food and then reuniting (fusion) at night to sleep, as demonstrated in Figure 3. Females are depicted by light forms, whereas males are depicted by dark forms, as shown in Figure 4. This one-of-a-kind method was incorporated into the algorithm to improve the efficiency of the search mechanism. BO is like other heuristics, and each solution in the population is termed a bonobo and the alpha bonobo (α bonobo) is the bonobo with the highest rank in the population's dominance hierarchy. More so, bonobos move forward through the positive phase (pp) and negative phase (np) of their phase probability, which indicates either population diversity or selection pressure (np). Positive phase count (ppc) and negative phase count (npc) are the counts of the consecutive number of iterations of pp and np, respectively. To reproduce young bonobos, the bonobo uses four main mating strategies: promiscuous and restrictive, consortship, and extra-group mating [53].

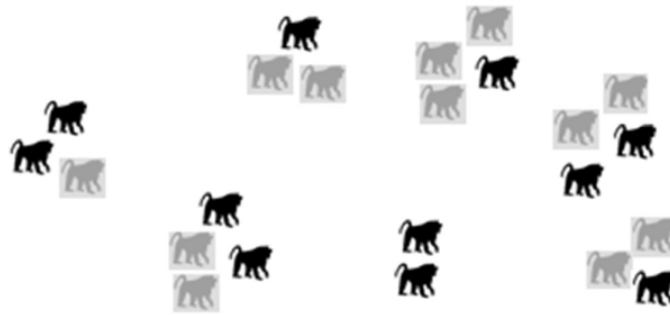


Figure 3. Bonobo social groups: both fission and fusion. Females are light forms; males are dark.

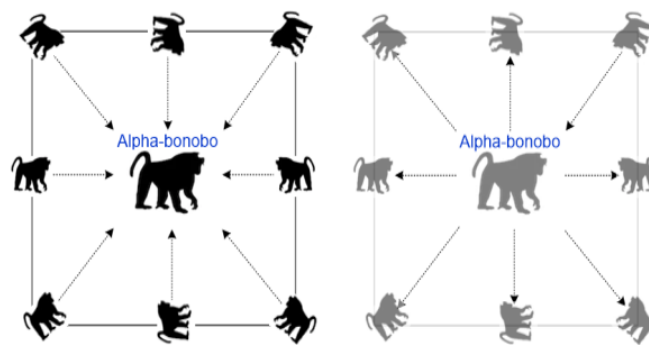


Figure 4. Movement directions of bonobos in pp (dark forms) and np (light forms) with higher probabilities.

The mating tactics alter depending on the phase condition (positive or negative). First, the positive phase (pp) depicts the state of the bonobo community, in which there is enough food, protection from other communities, breeding success, and genetic variation among bonobos. The odds for the first two types of mating, i.e., promiscuous and restricted mating, are higher during this phase. An oestrus female is available for both alpha bonobos (the highest-ranking male among all bonobos in a society) and other lower-ranking males in the promiscuous kind of mating. In the event of restricted mating, however, only the higher-ranking males are allowed to join. Consortship mating and extra-group mating are more likely in the case of negative phase (np), which signals a negative state in the society. A pair is separated from their natal community and spend their time together in a type of mating known as consortship. They rejoin with their community after a few days or weeks. In the case of extra-group mating, a female bonobo is found engaging in mating with males from other communities. Furthermore, compared to the other, the likelihood of extra-group mating is quite low. In the proposed BO, these physical processes are artificially recreated with the help of mathematics for optimization. The flowchart of the proposed bonobo optimizer algorithm is shown in Figure 5.

4.1. Promiscuous and Restrictive Mating Approach

The bonobos' mating approach is determined by the phase probability parameter (pp). The value of pp is set to 0.5 at the start, and it is changed after each iteration. If a random number r with a value between 0 and 1 is discovered to be less than or equal to pp, a new bonobo is born, as indicated in the following formula [53].

$$n_b_j = b_j^i + r_1 s^\alpha (\alpha_j^b - b_j^i) + (1 - r_1) s^s \text{flag} (b_j^i - b_j^p) \quad (14)$$

where b is bonobo; n_b_j and α_j^b are the new offspring and α bonobo j th variables, respectively; j is an integer that ranges from 1 to d (variables number); and the variables b_j^i and b_j^p represent the i th and p th bonobo variable values, respectively. A value in the range of

0 to 1 is represented by r_1 . The sharing coefficients for the α bonobo and p th bonobos are s^a and s^s , respectively. The *flag* argument has a value between -1 and 1 . When the optimal solution of the i th bonobo produces a better result than the p th bonobos, this is known as promiscuous mating. In this case, the *flag* is given one point. Restrictive mating is a different term for the same thing. The *flag* and α bonobo are given -1 in this regard.

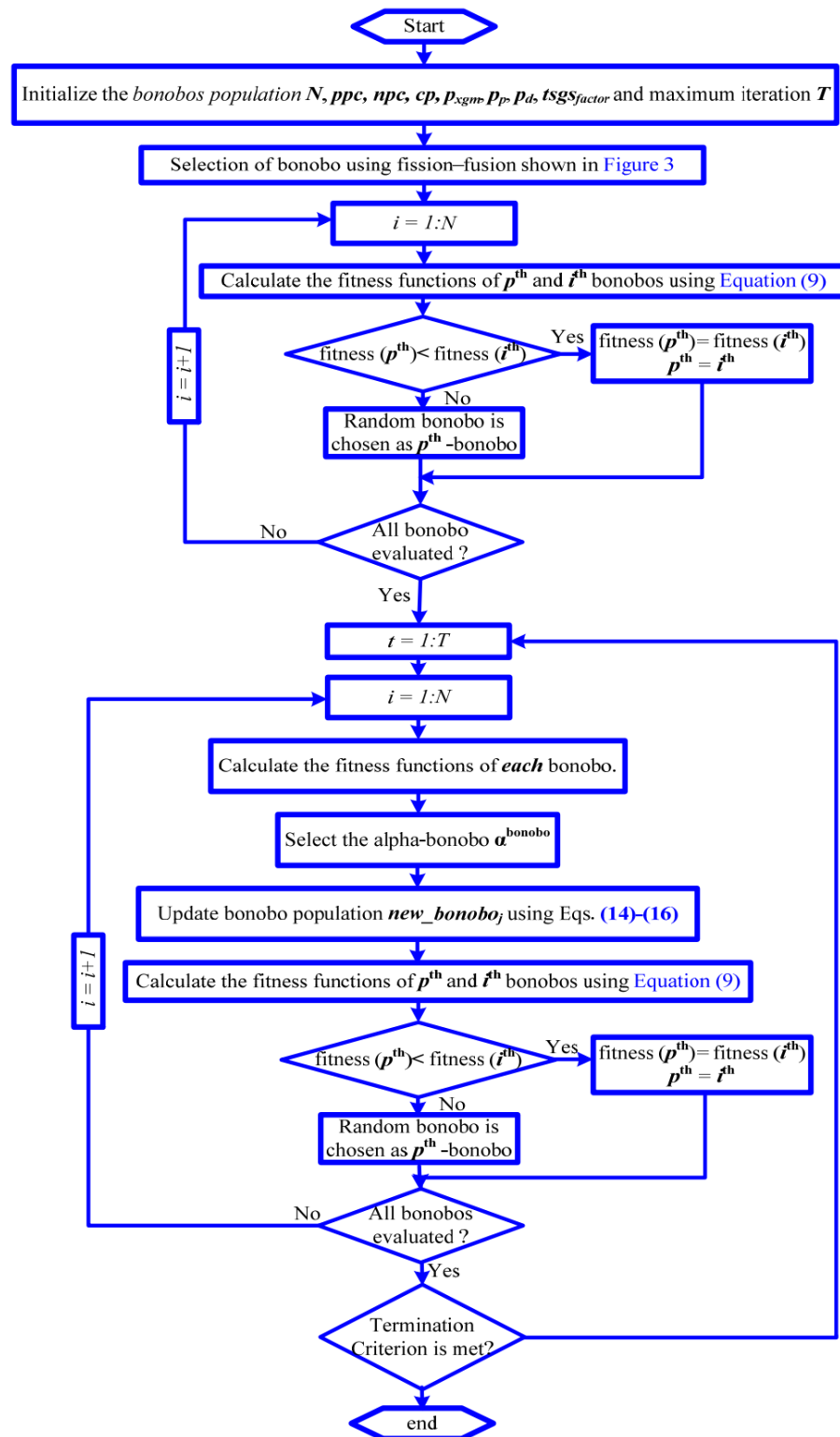


Figure 5. The bonobo optimizer algorithm flowchart.

4.2. Consortship and Extra-Group Mating Strategies

When phase p_p is less than the random integer r , this type of mating occurs. If r_2 is equal to or less than the probability of extra-group mating (p_{xgm}), the solution is updated by extra-group mating [53].

$$n_{-}b_j = \begin{cases} b_j^i + e^{(r_3^2+r_3-2r_3^{-1})} (Var_max_j - b_j^i) & \alpha_j^{bonobo} \geq b_j^i \\ b_j^i - e^{(-r_4^2+2r_4-2r_4^{-1})} (b_j^i - Var_min_j) & r_3 \leq p_d \\ b_j^i - e^{(r_3^2+r_3-2r_3^{-1})} (b_j^i - Var_min_j) & \alpha_j^{bonobo} \leq b_j^i \\ b_j^i + e^{(-r_4^2+2r_4-2r_4^{-1})} (Var_max_j - b_j^i) & r_3 \geq p_d \end{cases} \quad (15)$$

The p_d is set to 0.5 and is gradually updated based on the nature of evolution. The p_d optimizes the search process to find the best result. The lower and higher boundaries of the j th variable are represented by Var_min_j and Var_max_j respectively.

When the value of r_2 is greater than the value of p_{xgm} , a new offspring is produced utilizing the consortship mating strategy, which is as follows [53]:

$$n_{-}b_j = \begin{cases} n_{-}b_j + e^{r_5} flag(1 + r_1) (b_j^i - b_j^p) & r_6 \leq p_d \\ b_j^p & otherwise \end{cases} \quad (16)$$

where $r_1, r_2, r_3, r_4,$ and r_5 are random numbers ranging from 0 to 1.

5. Simulation Results and Discussion

The bonobo optimizer (BO) was proposed and applied to the optimal design/sizing of the proposed hybrid energy system including solar PV, WT, diesel, and batteries to electrify an urban area called Al Sulaymaniyah village in Arar in the northern area of Saudi Arabia. To validate the performance of the BO, it was compared to four other artificial intelligence algorithms—BBBC, crow search, GA, and BOA—to search for the optimal solution of the proposed HRES with a quick convergence rate. MATLAB R2019b/Windows 10/64-bit was used for the implementation of this optimization problem with 500 iterations and 50 runs for all five artificial intelligence algorithms. The average hourly solar irradiance and wind speed values were considered in this study. The parameters used in this study for all artificial intelligence algorithms are summarized in Table 1.

Table 1. The parameters used in this study for all four artificial intelligence algorithms.

Algorithm	Main Parameters	Value
BO	Rate of change in phase probability	0.0035
	Sharing coefficient for selected bonobo	1.3
	Sharing coefficient for alpha bonobo	1.25
	Extra-group mating probability	0.001
BBBC	Energy of rabbit	2
	Population size	100
Crow search	Awareness probability	0.1
	Flight length	2
GA	Population	100
	Selection	Roulette wheel
	Mutation rate	0.2
	Crossover rate	0.8
BOA	Sensory modality	0.01
	Power exponent	0.1

The simulation results of the proposed BO compared to the four artificial intelligence algorithms are shown in Table 2 for achieving the optimal design/sizing of the proposed

HRES with an LPSP of 0%. The proposed HRES contains PV, WT, a diesel generator, and batteries. As shown in Table 2, the BO had the best performance, followed by BOA, compared to the other three artificial intelligence algorithms (BBBC, crow, and GA), where it achieved the optimal solution/sizing of the proposed HRES with the lowest ASC. This is also demonstrated in Figure 6, which shows the optimal ASC using BO compared to the other four metaheuristic techniques for LPSP = 0%. In addition, the worst solution of the BOA was better than the optimal solution of the BBBC, crow, and GA algorithms. The optimal design/sizing of the PV, WT, diesel generator, and batteries for all five metaheuristic algorithms is shown in Figure 7. Moreover, Figure 8a,b shows the five performance indicators (optimal solution, worst solution, mean, median, and STDEV) that were used to evaluate the performance of all five metaheuristic algorithms. As revealed in Figure 8, BO had the best performance compared to the other four metaheuristic algorithms in terms of optimal solution, worst solution, mean, median, and STDEV. The BO and crow search algorithms achieved the smallest STDEV for the proposed HRES. A low STDEV means that the optimal solutions are concentrated around the mean. Therefore, they have fewer oscillations around steady state and follow the optimal solution quickly, taking less time to converge. On the other hand, BBBC and GA had the lowest performance based on these five performance indicators. They had high standard deviation. This means that the optimal solutions were highly dispersed. Therefore, they had obvious oscillations around the optimal solution and took more time to converge.

Table 2. Simulation results of the proposed BO compared to the other four artificial intelligence techniques for achieving the optimal design/sizing of the proposed HRES with 0% LPSP.

Algorithm	Performance Indicators	P_{PV} (kW)	P_{WT} (kW)	$P_{Bat.}$ (kW)	P_{Diesel} (kW)	ASC (USD/year)	REF (%)
BO	Optimal	341.3	403.9	499.8	215.9	149,977.2	82.7
	Worst	342	353.7	500	220.12	150,320.8	81.04
	Mean	340.62	400.36	499.83	215.84	150,033.1	82.61
	STDEV	5.97	12.75	0.2996	2.894	95.397	0.4021
BBBC	Optimal	397.85	348.4	923.9	229.1	150,883.5	64.55
	Worst	293.95	434.95	1436.3	248.06	158,884.5	70.52
	Mean	372.75	364.27	844.21	239.71	154,138.5	86.67
	STDEV	72.14	69.41	293.67	7.45	2007.99	10.379
Crow Search	Optimal	341.3	403.98	499.22	215.93	151,618.8	82.74
	Worst	358.7	405.75	498.86	221.74	151,832.6	83.046
	Mean	341.84	405.04	499.11	216	151,640.4	82.774
	STDEV	4.568	2.931	0.3925	0.8840	50.772	0.0984
GA	Optimal	370.21	311.51	1027.5	210.8	150,718	85.22
	Worst	496.29	260.45	1355.8	204.24	154,770	88.27
	Mean	375.56	346.95	940.64	219.09	151,944.6	85.55
	STDEV	45.92	52.921	161.35	21.43	927.45	1.6267
BOA	Optimal	361.28	373.70	950.01	227.34	150,236.4	63.32
	Worst	352.07	331.31	657.54	228.07	151,968.8	61.28
	Mean	343.87	353.63	850.27	214.06	151,130.5	66.93
	STDEV	26.359	27.982	161.531	11.461	422.106	6.2367

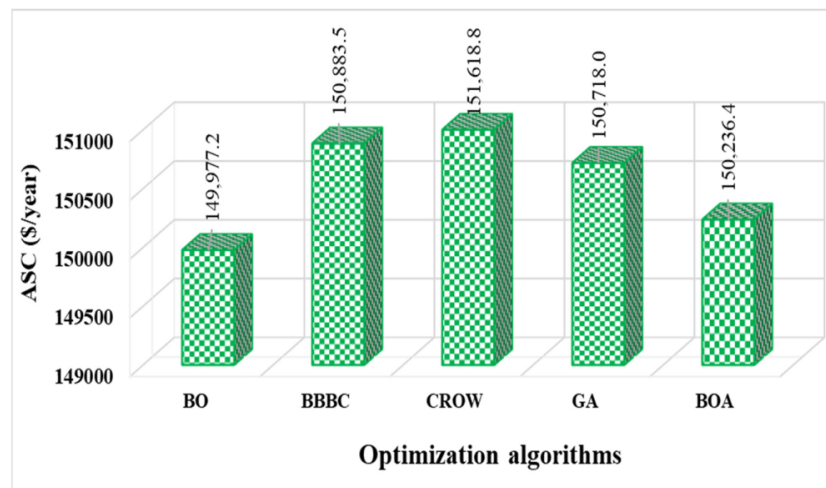


Figure 6. The optimal ASC using BO compared to the other four metaheuristic techniques for LPSP = 0%.

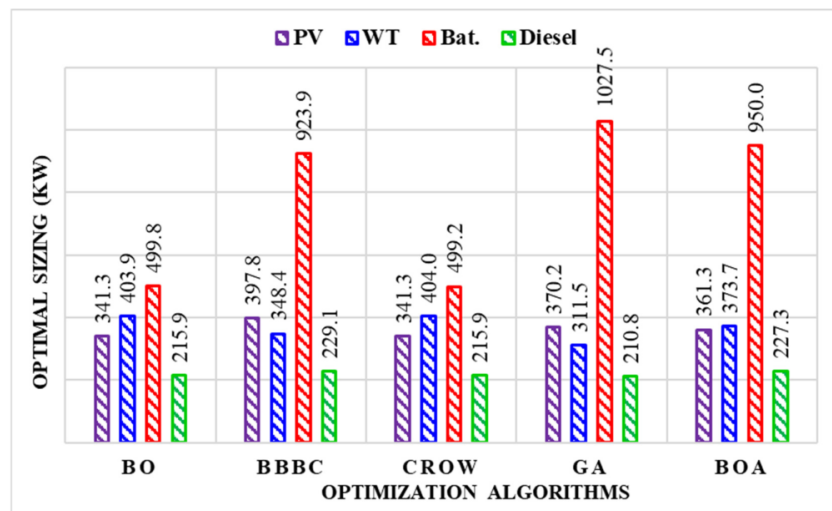
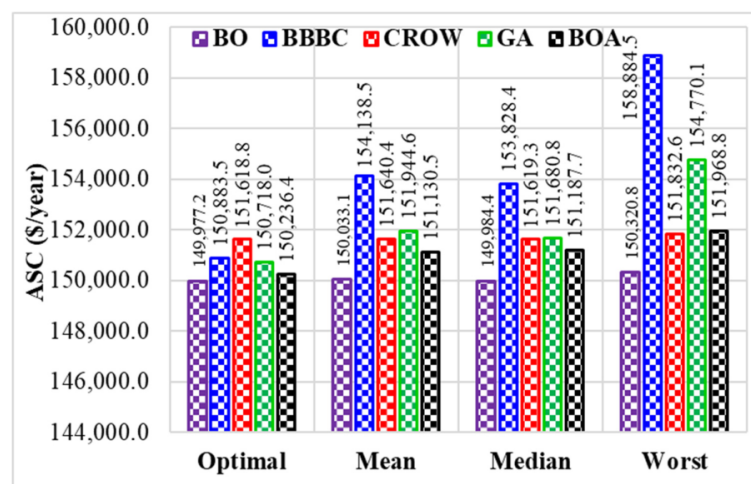


Figure 7. The optimal sizing of the solar PV, WT, diesel generator, and batteries for all five metaheuristic algorithms.



(a)

Figure 8. Cont.

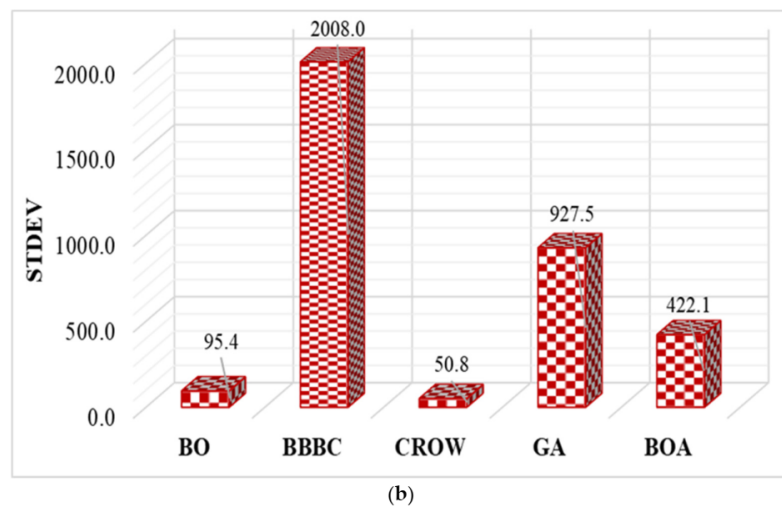


Figure 8. The performance indicators with all eight metaheuristic algorithms: (a) optimal, worst, mean, median, and (b) STDEV.

Figure 9 presents the ASC versus the run number for the BO technique in comparison to the other four metaheuristic techniques. This graph proved that BO followed by BOA and crow search followed the global solution and achieved the optimal sizing of the HRES with less ASC and fewer oscillations. This is due to the fact that their standard deviation was low. This means that the optimal solutions were concentrated around the mean. Therefore, they had fewer oscillations around steady state, as shown in Figure 9, and followed the optimal solution quickly, taking less time to converge, as shown in Figure 10. On the other hand, BBBC and GA were trapped to the local solution with obvious oscillations around the steady state, as shown in Figure 9. On the other hand, Figure 10 presents the convergence rate of all five metaheuristic algorithms: BO, BBBC, crow search, GA, and BOA. This figure shows that the BO followed the global solution with a faster convergence rate than the other four metaheuristic algorithms (BBBC, crow search, GA, and BOA). This figure also emphasizes that both BBBC and GA may have been trapped to the local solution and had the lowest convergence rate compared to the other metaheuristic techniques.

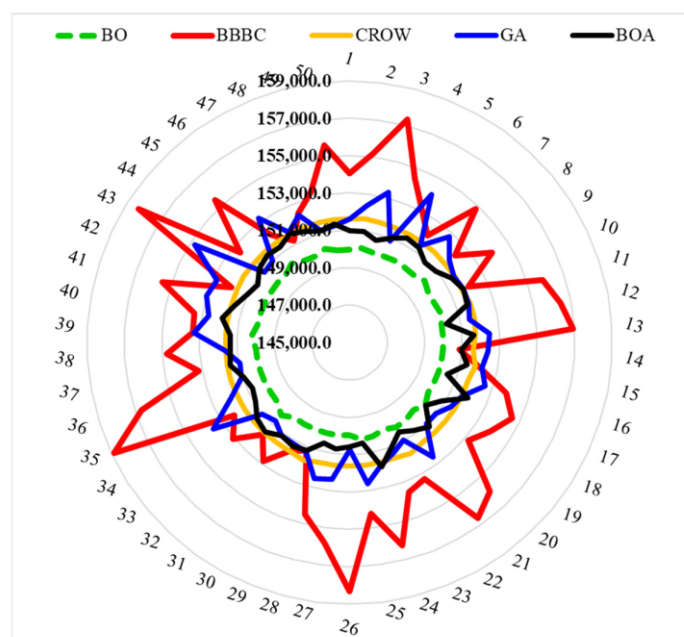


Figure 9. The ASC versus run number using BO compared to the other four metaheuristic techniques.

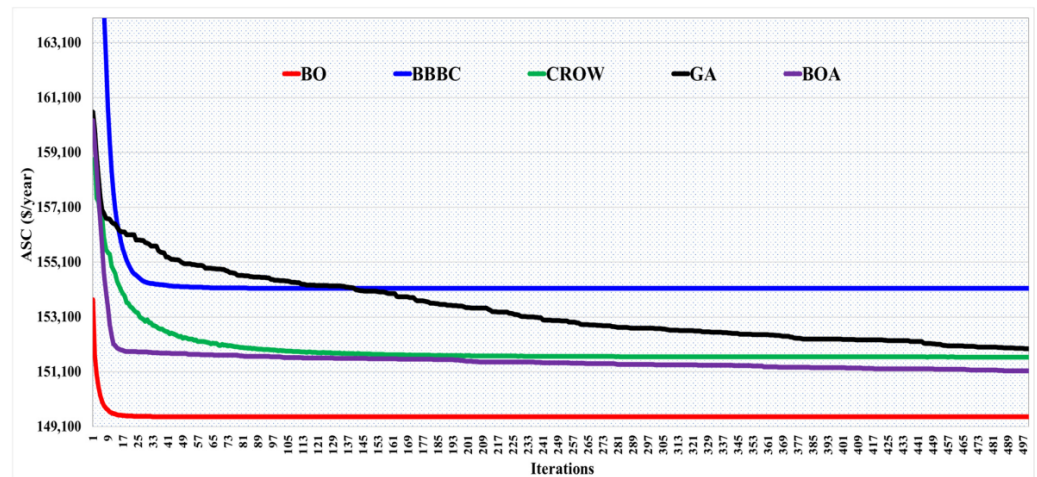


Figure 10. The convergence time of BO compared to the other four metaheuristic techniques.

Under different values of diesel prices (USD/liter), the simulation findings of the proposed BO are introduced in Table 3 for achieving the optimal design/sizing of the proposed HRES that includes solar PV, WT, a diesel generator, and batteries. As the diesel price increased, the optimal design/sizing of the diesel generator decreased, and at the same time, the renewable sizes (WT and PV) and REF% increased, as shown in Table 3. This is also evident in Figure 11a,b. On the other hand, the CO₂ emissions (kg/yr) reduced dramatically from 454,729.3 to 94,232.7 kg/yr with the increase in diesel prices from 0.1 to 1.5 USD/liter, as shown in Figure 11c. In addition, both ASC and fuel cost doubled as the diesel price increased from 0.1 to 1.5 USD/liter.

Table 3. Simulation results of the proposed BO algorithm under different diesel prices for achieving the optimal sizing of the proposed HRES.

Diesel Price (USD/Liter)	PV	WT	Bat.	Diesel	REF	Surplus	Diesel Hours	Fuel cost (USD/yr)	CO ₂ (kg/yr)	ASC (USD/yr)
0.1	315.7	7.1	109.5	289.3	43.1	6.6	6021.0	30,660.6	454,729.3	98,185.6
0.2	275.9	255.7	287.1	226.6	71.6	11.0	3520.0	29,593.7	229,691.9	116,353.0
0.3	288.8	312.6	493.1	215.8	77.8	68.9	2669.0	33,386.3	178,479.0	129,834.4
0.4	341.0	354.9	499.8	222.8	81.0	54.9	2242.0	38,296.3	152,589.4	140,686.4
0.5	341.3	403.9	499.8	215.9	82.7	3.5	2020.0	42,722.8	138,529.7	149,977.2
0.6	327.8	422.3	499.8	202.2	83.1	20.3	1992.0	48,897.7	135,260.3	158,364.8
0.7	347.3	455.7	499.5	187.7	84.5	56.3	1844.0	50,872.3	123,745.5	166,060.2
0.8	372.6	482.5	482.0	176.1	85.5	15.7	1724.0	52,893.3	115,260.1	173,061.2
0.9	372.6	482.5	482.0	176.1	85.5	17.8	1724.0	59,505.0	115,260.1	179,672.8
1.0	402.8	496.8	489.2	134.7	87.1	16.2	1659.0	54,689.9	101,971.3	185,830.4
1.1	402.5	496.9	489.0	134.7	87.1	55.9	1660.0	60,189.7	102,002.2	191,319.3
1.2	403.1	497.7	487.3	134.5	87.1	21.7	1657.0	65,512.1	101,843.4	196,821.0
1.3	404.9	498.9	499.8	126.6	87.5	64.2	1634.0	67,803.4	98,737.1	202,402.6
1.4	451.4	499.7	500.0	121.4	88.1	2.5	1583.0	69,060.1	94,232.8	207,520.9
1.5	451.4	499.7	500.0	121.4	88.1	88.3	1583.0	73,992.8	94,232.7	212,453.8

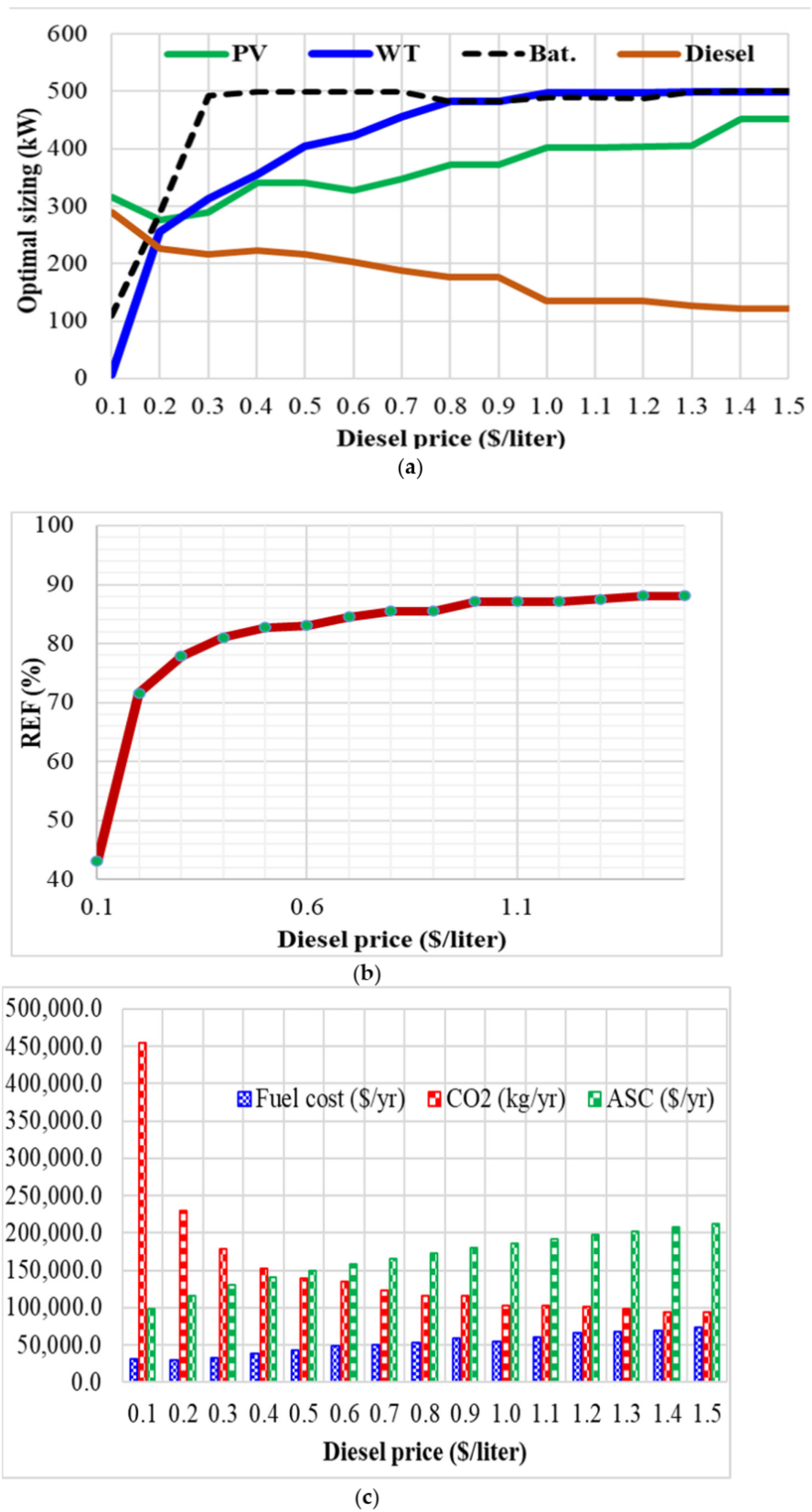


Figure 11. Simulation results using the proposed BO algorithm under different diesel prices of (a) optimal design/sizing of the solar PV, WT, diesel generator, and batteries; (b) REF %; (c) ASC, fuel cost, and CO₂ emissions.

6. Conclusions

The bonobo optimizer (BO) was proposed and applied for the optimal design/sizing of a hybrid renewable energy system (HRES) including PV, WT, diesel, and batteries to electrify an urban area called Al Sulaymaniyah village, in Arar in the northern part of Saudi Arabia. For the validation purposes, the BO was compared to four metaheuristic algorithms—BBBC, crow search, GA, and BOA—to find the optimal solution for the HRES with a quick convergence rate. These performance indicators (optimal solution, worst solution, mean, median, STDEV, and convergence rate) were used to discern the most appropriate performance among these five metaheuristic algorithms. The simulation findings revealed that the BO outperformed the other four metaheuristic algorithms—BBBC, crow search, GA, and BOA—where it achieved the optimal HRES solution/sizing with minimum ASC (USD 149,977.2), quick convergence time, and fewer oscillations around steady state. Both the BBBC and GA algorithms trapped into the local solution and failed to capture the global solution. In addition, they had high standard deviation, which means that the optimal solutions were highly dispersed. Hence, they had obvious oscillations around the optimal solution and took longer to converge. On the other hand, both BO and crow search had low standard deviation, which means that the optimal solutions were concentrated around the mean. These results prove the efficacy and robustness of the proposed BO algorithm compared to the other four metaheuristic optimization algorithms.

Author Contributions: Conceptualization, H.M.H.F. and A.A.A.-S.; methodology, H.M.H.F. and A.A.A.-S.; software, H.M.H.F. and A.A.A.-S.; validation, H.M.H.F. and A.A.A.-S.; formal analysis, H.M.H.F., A.A.A.-S., A.M.A.-S., A.A., A.M.N. and T.K.; investigation, H.M.H.F. and A.A.A.-S.; resources, A.M.A.-S., A.M.N., and A.A.; data curation, H.M.H.F. and A.A.A.-S.; writing—original draft preparation, H.M.H.F.; writing—review and editing, A.M.A.-S., A.A., A.M.N. and T.K.; visualization, H.M.H.F., A.A.A.-S. and A.M.N.; supervision, A.M.A.-S.; project administration, A.M.A.-S.; funding acquisition, A.M.A.-S. All authors have read and agreed to the published version of the manuscript.

Funding: This research received no external funding.

Acknowledgments: The authors would like to acknowledge the Researchers Supporting Project number (RSP-2021/337), King Saud University, Riyadh, Saudi Arabia.

Conflicts of Interest: The authors declare no conflict of interest.

References

1. Eltamaly, A.M.; Farh, H.M.H.; Al Saud, M.S. Impact of PSO reinitialization on the accuracy of dynamic global maximum power detection of variant partially shaded PV systems. *Sustainability* **2019**, *11*, 2091. [[CrossRef](#)]
2. Alturki, F.A.; Al-Shamma'a, A.A.; Farh, H.M.H. Simulations and dSPACE Real-Time Implementation of Photovoltaic Global Maximum Power Extraction under Partial Shading. *Sustainability* **2020**, *12*, 3652. [[CrossRef](#)]
3. Gao, K.; Wang, T.; Han, C.; Xie, J.; Ma, Y.; Peng, R. A Review of Optimization of Microgrid Operation. *Energies* **2021**, *14*, 2842. [[CrossRef](#)]
4. Lian, J.; Zhang, Y.; Ma, C.; Yang, Y.; Chaima, E. A review on recent sizing methodologies of hybrid renewable energy systems. *Energy Convers. Manag.* **2019**, *199*, 112027. [[CrossRef](#)]
5. Acuna, L.G.; Padilla, R.V.; Mercado, A.S. Measuring reliability of hybrid photovoltaic-wind energy systems: A new indicator. *Renew. Energy* **2017**, *106*, 68–77. [[CrossRef](#)]
6. Gong, X.; Dong, F.; Mohamed, M.A.; Abdalla, O.M.; Ali, Z.M. A secured energy management architecture for smart hybrid microgrids considering PEM-fuel cell and electric vehicles. *IEEE Access* **2020**, *8*, 47807–47823. [[CrossRef](#)]
7. Alnowibet, K.; Annuk, A.; Dampage, U.; Mohamed, M.A. Effective Energy Management via False Data Detection Scheme for the Interconnected Smart Energy Hub–Microgrid System under Stochastic Framework. *Sustainability* **2021**, *13*, 11836. [[CrossRef](#)]
8. Belmili, H.; Haddadi, M.; Bacha, S.; Almi, M.F.; Bendib, B. Sizing stand-alone photovoltaic–wind hybrid system: Techno-economic analysis and optimization. *Renew. Sustain. Energy Rev.* **2014**, *30*, 821–832. [[CrossRef](#)]
9. Zhao, X.; Wang, C.; Su, J.; Wang, J. Research and application based on the swarm intelligence algorithm and artificial intelligence for wind farm decision system. *Renew. Energy* **2019**, *134*, 681–697. [[CrossRef](#)]
10. Chen, H.-C. Optimum capacity determination of stand-alone hybrid generation system considering cost and reliability. *Appl. Energy* **2013**, *103*, 155–164. [[CrossRef](#)]
11. Shayeghi, H.; Hashemi, Y. Application of fuzzy decision-making based on INSGA-II to designing PV–wind hybrid system. *Eng. Appl. Artif. Intell.* **2015**, *45*, 1–17. [[CrossRef](#)]

12. Zhang, Y.; Ma, C.; Lian, J.; Pang, X.; Qiao, Y.; Chaima, E. Optimal photovoltaic capacity of large-scale hydro-photovoltaic complementary systems considering electricity delivery demand and reservoir characteristics. *Energy Convers. Manag.* **2019**, *195*, 597–608. [[CrossRef](#)]
13. Delgado-Antillón, C.; Domínguez-Navarro, J. Probabilistic siting and sizing of energy storage systems in distribution power systems based on the islanding feature. *Electr. Power Syst. Res.* **2018**, *155*, 225–235. [[CrossRef](#)]
14. Menshshari, A.; Ghiamy, M.; Mousavi, M.M.; Bagal, H. Optimal design of hybrid water-wind-solar system based on hydrogen storage and evaluation of reliability index of system using ant colony algorithm. *Int. Res. J. Appl. Basic Sci.* **2013**, *4*, 3582–3600.
15. Mohamed, A.F.; Elarini, M.M.; Othman, A.M. A new technique based on Artificial Bee Colony Algorithm for optimal sizing of stand-alone photovoltaic system. *J. Adv. Res.* **2014**, *5*, 397–408. [[CrossRef](#)]
16. Maleki, A.; Askarzadeh, A. Optimal sizing of a PV/wind/diesel system with battery storage for electrification to an off-grid remote region: A case study of Rafsanjan, Iran. *Sustain. Energy Technol. Assess.* **2014**, *7*, 147–153. [[CrossRef](#)]
17. Sanajaoba, S.; Fernandez, E. Maiden application of Cuckoo Search algorithm for optimal sizing of a remote hybrid renewable energy system. *Renew. Energy* **2016**, *96*, 1–10. [[CrossRef](#)]
18. Berrueta, A.; Heck, M.; Jantsch, M.; Ursúa, A.; Sanchis, P. Combined dynamic programming and region-elimination technique algorithm for optimal sizing and management of lithium-ion batteries for photovoltaic plants. *Appl. Energy* **2018**, *228*, 1–11. [[CrossRef](#)]
19. Zhou, W.; Lou, C.; Li, Z.; Lu, L.; Yang, H. Current status of research on optimum sizing of stand-alone hybrid solar-wind power generation systems. *Appl. Energy* **2010**, *87*, 380–389. [[CrossRef](#)]
20. Farh, H.M.; Al-Shaalan, A.M.; Eltamaly, A.M.; Al-Shamma'A, A.A. A Novel Crow Search Algorithm Auto-Drive PSO for Optimal Allocation and Sizing of Renewable Distributed Generation. *IEEE Access* **2020**, *8*, 27807–27820. [[CrossRef](#)]
21. Veilleux, G.; Potisat, T.; Pezim, D.; Ribback, C.; Ling, J.; Krysztofiński, A.; Ahmed, A.; Papenheim, J.; Pineda, A.M.; Sembian, S. Techno-economic analysis of microgrid projects for rural electrification: A systematic approach to the redesign of Koh Jik off-grid case study. *Energy Sustain. Dev.* **2020**, *54*, 1–13. [[CrossRef](#)]
22. Odou, O.D.T.; Bhandari, R.; Adamou, R. Hybrid off-grid renewable power system for sustainable rural electrification in Benin. *Renew. Energy* **2020**, *145*, 1266–1279. [[CrossRef](#)]
23. Amir Khalili, S.; Zahedi, A. Techno-economic analysis of a stand-alone hybrid wind/fuel cell microgrid system: A case study in Kouhin region in Qazvin. *Fuel Cells* **2018**, *18*, 551–560. [[CrossRef](#)]
24. Luna-Rubio, R.; Trejo-Perea, M.; Vargas-Vázquez, D.; Ríos-Moreno, G. Optimal sizing of renewable hybrids energy systems: A review of methodologies. *Sol. Energy* **2012**, *86*, 1077–1088. [[CrossRef](#)]
25. Jakhani, A.Q.; Othman, A.-K.; Rigit, A.R.H.; Samo, S.R.; Kamboh, S.A. A novel analytical model for optimal sizing of standalone photovoltaic systems. *Energy* **2012**, *46*, 675–682. [[CrossRef](#)]
26. Hung, D.Q.; Mithulanathan, N.; Bansal, R. Analytical strategies for renewable distributed generation integration considering energy loss minimization. *Appl. Energy* **2013**, *105*, 75–85. [[CrossRef](#)]
27. Sanjel, N.; Baral, B.; Acharya, M.; Gautam, S. Analytical modelling for optimized selection between renewable energy systems and the conventional grid expansion. *J. Phys. Conf. Ser.* **2019**, *1266*, 012014. [[CrossRef](#)]
28. Sinha, S.; Chandel, S. Review of recent trends in optimization techniques for solar photovoltaic-wind based hybrid energy systems. *Renew. Sustain. Energy Rev.* **2015**, *50*, 755–769. [[CrossRef](#)]
29. Markvart, T. Sizing of hybrid photovoltaic-wind energy systems. *Sol. Energy* **1996**, *57*, 277–281. [[CrossRef](#)]
30. Clúa, J.G.G.; Mantz, R.J.; De Battista, H. Optimal sizing of a grid-assisted wind-hydrogen system. *Energy Convers. Manag.* **2018**, *166*, 402–408. [[CrossRef](#)]
31. Upadhyay, S.; Sharma, M. A review on configurations, control and sizing methodologies of hybrid energy systems. *Renew. Sustain. Energy Rev.* **2014**, *38*, 47–63. [[CrossRef](#)]
32. Cabral, C.V.T.; Oliveira Filho, D.; Diniz, A.S.A.C.; Martins, J.H.; Toledo, O.M.; Lauro de Vilhena, B. A stochastic method for stand-alone photovoltaic system sizing. *Sol. Energy* **2010**, *84*, 1628–1636. [[CrossRef](#)]
33. Khatib, T.; Ibrahim, I.A.; Mohamed, A. A review on sizing methodologies of photovoltaic array and storage battery in a standalone photovoltaic system. *Energy Convers. Manag.* **2016**, *120*, 430–448. [[CrossRef](#)]
34. Giallanza, A.; Porretto, M.; Puma, G.L.; Marannano, G. A sizing approach for stand-alone hybrid photovoltaic-wind-battery systems: A Sicilian case study. *J. Clean. Prod.* **2018**, *199*, 817–830. [[CrossRef](#)]
35. Rullo, P.; Braccia, L.; Luppi, P.; Zumoffen, D.; Feroldi, D. Integration of sizing and energy management based on economic predictive control for standalone hybrid renewable energy systems. *Renew. Energy* **2019**, *140*, 436–451. [[CrossRef](#)]
36. Mahmoudimehr, J.; Shabani, M. Optimal design of hybrid photovoltaic-hydroelectric standalone energy system for north and south of Iran. *Renew. Energy* **2018**, *115*, 238–251. [[CrossRef](#)]
37. Portero, U.; Velázquez, S.; Carta, J.A. Sizing of a wind-hydro system using a reversible hydraulic facility with seawater. A case study in the Canary Islands. *Energy Convers. Manag.* **2015**, *106*, 1251–1263. [[CrossRef](#)]
38. Elbaz, A.; Güneşer, M.T. Using crow algorithm for optimizing size of wind power plant/hybrid PV in Libya. In Proceedings of the 2019 3rd International Symposium on Multidisciplinary Studies and Innovative Technologies (ISMSIT), Ankara, Turkey, 11–13 October 2019; pp. 1–4.
39. Maleki, A.; Khajeh, M.G.; Ameri, M. Optimal sizing of a grid independent hybrid renewable energy system incorporating resource uncertainty, and load uncertainty. *Int. J. Electr. Power Energy Syst.* **2016**, *83*, 514–524. [[CrossRef](#)]

40. Mayer, M.J.; Szilágyi, A.; Gróf, G. Environmental and economic multi-objective optimization of a household level hybrid renewable energy system by genetic algorithm. *Appl. Energy* **2020**, *269*, 115058. [[CrossRef](#)]
41. Dufo-López, R.; Bernal-Agustín, J.L.; Yusta-Loyo, J.M.; Domínguez-Navarro, J.A.; Ramírez-Rosado, I.J.; Lujano, J.; Aso, I. Multi-objective optimization minimizing cost and life cycle emissions of stand-alone PV–wind–diesel systems with batteries storage. *Appl. Energy* **2011**, *88*, 4033–4041. [[CrossRef](#)]
42. Das, M.; Singh, M.A.K.; Biswas, A. Techno-economic optimization of an off-grid hybrid renewable energy system using metaheuristic optimization approaches—case of a radio transmitter station in India. *Energy Convers. Manag.* **2019**, *185*, 339–352. [[CrossRef](#)]
43. Abedi, S.; Alimardani, A.; Gharehpetian, G.; Riahy, G.; Hosseinian, S. A comprehensive method for optimal power management and design of hybrid RES-based autonomous energy systems. *Renew. Sustain. Energy Rev.* **2012**, *16*, 1577–1587. [[CrossRef](#)]
44. Zhao, J.; Yuan, X. Multi-objective optimization of stand-alone hybrid PV-wind-diesel-battery system using improved fruit fly optimization algorithm. *Soft Comput.* **2016**, *20*, 2841–2853. [[CrossRef](#)]
45. Shi, B.; Wu, W.; Yan, L. Size optimization of stand-alone PV/wind/diesel hybrid power generation systems. *J. Taiwan Inst. Chem. Eng.* **2017**, *73*, 93–101. [[CrossRef](#)]
46. Tabak, A.; Kayabasi, E.; Guneser, M.T.; Ozkaymak, M. Grey wolf optimization for optimum sizing and controlling of a PV/WT/BM hybrid energy system considering TNPC, LPSP, and LCOE concepts. *Energy Sources Part A Recovery Util. Environ. Eff.* **2019**, 1–21. Available online: <https://www.tandfonline.com/doi/abs/10.1080/15567036.2019.1668880?journalCode=ueso20> (accessed on 27 December 2021).
47. Ahmadi, S.; Abdi, S. Application of the Hybrid Big Bang–Big Crunch algorithm for optimal sizing of a stand-alone hybrid PV/wind/battery system. *Sol. Energy* **2016**, *134*, 366–374. [[CrossRef](#)]
48. Fetanat, A.; Khorasaninejad, E. Size optimization for hybrid photovoltaic–wind energy system using ant colony optimization for continuous domains based integer programming. *Appl. Soft Comput.* **2015**, *31*, 196–209. [[CrossRef](#)]
49. Injeti, S.K. Butterfly optimizer-assisted optimal integration of REDG units in hybrid AC/DC distribution micro-grids based on minimum operational area. *J. Electr. Syst. Inf. Technol.* **2021**, *8*, 13. [[CrossRef](#)]
50. Alturki, F.A.; Al-Shamma'a, A.A.; Farh, H.M.; AlSharabi, K. Optimal sizing of autonomous hybrid energy system using supply-demand-based optimization algorithm. *Int. J. Energy Res.* **2021**, *45*, 605–625. [[CrossRef](#)]
51. Alturki, F.A.; Farh, H.M.H.; Al-Shamma'a, A.A.; AlSharabi, K. Techno-Economic Optimization of Small-Scale Hybrid Energy Systems Using Manta Ray Foraging Optimizer. *Electronics* **2020**, *9*, 2045. [[CrossRef](#)]
52. Al-Shamma'a, A.A.; Alturki, F.A.; Farh, H.M. Techno-economic assessment for energy transition from diesel-based to hybrid energy system-based off-grids in Saudi Arabia. *Energy Transit.* **2020**, *4*, 31–43. [[CrossRef](#)]
53. Das, A.K.; Pratihar, D.K. A new bonobo optimizer (BO) for real-parameter optimization. In Proceedings of the 2019 IEEE Region 10 Symposium (TENSymp), Kolkata, India, 7–9 June 2019.